Weierstraß-Institut
für Angewandte Analysis und Stochastik

Leibniz-Institut im Forschungsverbund Berlin e. V.

Preprint ISSN 2198-5855

Micro-geometry effects on the nonlinear effective yield strength response of magnetorheological fluids

Grigor Nika[1], Bogdan Vernescu[2]

submitted: January 7, 2020

[1] Weierstrass Institute
Mohrenstr. 39
10117 Berlin
Germany
E-Mail: grigor.nika@wias-berlin.de

[2] Department of Mathematical Sciences
Worcester Polytechnic Institute
100 Institute Rd
Worcester, MA 01609
USA
E-Mail: vernescu@wpi.edu

No. 2673

Berlin 2020

2010 *Mathematics Subject Classification.* 35J57, 35J60, 35M12, 76T20.

Key words and phrases. Magnetorheological fluids, chain structures, surface-to-volume effects.

G. Nika gratefully acknowledges the funding by the Deutsche Forschungsgemeinschaft (DFG, German Research Foundation) under Germany's Excellence Strategy – The Berlin Mathematics Research Center MATH+ (EXC-2046/1, project ID: 390685689) in project AA2-1.

Edited by
Weierstraß-Institut für Angewandte Analysis und Stochastik (WIAS)
Leibniz-Institut im Forschungsverbund Berlin e. V.
Mohrenstraße 39
10117 Berlin
Germany

Fax: +49 30 20372-303
E-Mail: preprint@wias-berlin.de
World Wide Web: http://www.wias-berlin.de/

Micro-geometry effects on the nonlinear effective yield strength response of magnetorheological fluids

Grigor Nika, Bogdan Vernescu

Abstract

We use the novel constitutive model in [15], derived using the homogenization method, to investigate the effect particle chain microstructures have on the properties of the magnetorheological fluid. The model allows to compute the constitutive coefficients for different geometries. Different geometrical realizations of chains can significantly change the magnetorheological effect of the suspension. Numerical simulations suggest that particle size is also important as the increase of the overall particle surface area can lead to a decrease of the overall magnetorheological effect while keeping the volume fraction constant.

1 Introduction

Magnetorhelogical (MR) fluids are a suspension of non-colloidal, ferromagnetic micron-sized particles in a non-magnetizable carrier fluid. They were discovered by J. Rabinow in 1948 [17].The ability of magnetorheological fluids [17] to transform from a liquid to a semi-solid state in a matter of milliseconds make them desirable for many applications [12, 5]. MR fluids are part of a larger class of suspensions of rigid particles, known as *smart* materials, for which their rheological properties can be controlled by the interaction with a magnetic or electric field. Hence, accurate models for numerical simulations constructed on a sound analytical basis are required.

Modeling of magnetorheological fluids has been, mostly, explored from a phenomenological point of view [3], by which a large class of admissible constitutive equations are derived, for which constitutive coefficients need to be either prescribed or experimentally obtained. These models also consider the Maxwell system decoupled from the fluid flow system. The theory of periodic homogenization, specifically designed to treat problems of highly heterogeneous and microstructure materials, was first used to derive effective models for magnetorheological fluids in [8, 9]. Improved effective models appeared a decade later in [16, 21] building upon the works in [8, 9]. The works in [8, 9, 16, 21] were further generalized in [15] where a new effective model was derived with a stress tensor that contained contributions both from the magnetic and the fluid components that depend on four different effective coefficients that can be numerically obtained from a series of local problems on the periodicity cell. In addition one can better understand how the geometry of the periodic cell can be used [15] to numerically obtain the added nonlinear effect chain-like structures [3] have in strengthening the magnetorheological effect.

Magnetizable particles show a wide range of unusual magnetic properties. Surface particle magnetization is different from bulk volume magnetization which strongly influences the magnetorheological effect. It is has been reported experimentally for magnetite nanoparticles (Fe_3O_4) an enhancement in saturation magnetization for particles of critical size up to $\sim 10\mathrm{nm}$ beyond which the magnetization reduces [20]. The latter is attributed to surface effects becoming predominant as surface to volume ratio increases. Similar effects where reported by [11, 10] regarding the effective conductive of composites with imperfect interfaces where the authors identified a critical radius R_{cr} for spherical particles such that for a polydisperse suspension of spheres when the mean radius lies below R_{cr} the effective conductivity of the composite lies below the conductivity of the enclosing matrix. In this work we are able to numerically capture a similar effect where the effective magnetic coefficient value decreases as the surface to volume ratio increases for particles with 15% volume fraction.

The paper is organized as follows: In Section 2 we introduce the hybrid model for magnetorheological suspensions as well as its effective counterpart together with the local problems. Section 3 is devoted to the numerical approximation of the local problems using viscosity and penalization methods. Section 4 computes the effective

DOI 10.20347/WIAS.PREPRINT.2673 Berlin 2020

magnetic coefficients for different geometrical realizations ranging from a single particle chain to a cluster of particles chains. Lastly, Section 5 contains conclusions and some remarks.

Notation

Throughout the paper we are going to be using the following notation: I indicates the $n \times n$ identity matrix, $\mathbb{I}_{\mathcal{C}}$ indicates the characteristics function over some set C, namely

$$\mathbb{I}_{\mathcal{C}}(\boldsymbol{s}) = \begin{cases} 0 & \text{if } \boldsymbol{s} \in C \\ +\infty & \text{otherwise,} \end{cases}$$

bold symbols indicate vectors in two or three dimensions, regular symbols indicate tensors, $e(\boldsymbol{u})$ indicates the strain rate tensor defined by $e(\boldsymbol{u}) = \frac{1}{2}\left(\nabla \boldsymbol{u} + \nabla \boldsymbol{u}^{\top}\right)$, where often times we will use subscript to indicate the variable of differentiation. The inner product between matrices is denoted by $A{:}B = tr(A^{\top}B) = \sum_{ij} A_{ij}\, B_{ji}$ and throughout the paper we employ the Einstein summation notation for repeated indices.

2 Modeling magneto-rheological suspensions

2.1 Hybrid modeling of magneto-rheological suspensions

We will next outline the coupled suspension model used in the homogenization process; it consists of the newtonian fluid with rigid particles coupled flow system, coupled with Maxwell's equations.

As in the periodic homogenization framework we first define the geometry of the suspension. We define $\Omega \subset \mathbb{R}^d$, $d \in \{2, 3\}$, to be a bounded open set with sufficiently smooth boundary $\partial\Omega$, $Y = [-1/2, 1/2)^d$ is the unit cube in $\mathbb{R}^d$, and $\mathbb{Z}^d$ is the set of all n–dimensional vectors with integer components. For every positive ϵ, let $N(\epsilon)$ be the set of all points $\ell \in \mathbb{Z}^d$ such that $\epsilon(\ell + Y)$ is strictly included in Ω and denote by $|N(\epsilon)|$ their total number. Let T be the closure of an open connected set with sufficiently smooth boundary, compactly included in Y. For every $\epsilon > 0$ and $\ell \in N^{\epsilon}$ we consider the set $T_{\ell}^{\epsilon} \subset\subset \epsilon(\ell + Y)$, where $T_{\ell}^{\epsilon} = \epsilon(\ell + T)$. The set T_{ℓ}^{ϵ} represents one of the rigid particles suspended in the fluid, and $S_{\ell}^{\epsilon} = \partial T_{\ell}^{\epsilon}$ denotes its surface (see Fig. 1). We now define the following subsets of Ω:

$$\Omega_{1\epsilon} = \bigcup_{\ell \in N^{\epsilon}} T_{\ell}^{\epsilon}\,, \quad \Omega_{2\epsilon} = \Omega \backslash \overline{\Omega}_{1\epsilon}.$$

In what follows T_{ℓ}^{ϵ} will represent the magnetizable rigid particles, $\Omega_{1\epsilon}$ is the domain occupied by the rigid particles and $\Omega_{2\epsilon}$ the domain occupied by the surrounding fluid of viscosity ν. We denote by $\partial\Omega$ the exterior boundary of Ω and by $\partial\Omega_{\epsilon} := \cup_{\ell} S_{\ell}^{\epsilon} \cup \partial\Omega$. By $\boldsymbol{n}$ we indicate the unit normal on the particle surface pointing outwards and by $[\![\cdot]\!]$ we indicate the jump discontinuity between the fluid and the rigid part.

The magnetorheological problem considered in [15] after non-dimensionalizing and assuming that the flow is at low Reynolds numbers is the following,

$$-\operatorname{div} \sigma^{\epsilon} = \mathbf{0}, \text{ where } \sigma^{\epsilon} = 2\, e(\boldsymbol{v}^{\epsilon}) - p^{\epsilon} I \qquad \text{in } \Omega_{2\epsilon}, \tag{1a}$$

$$\operatorname{div} \boldsymbol{v}^{\epsilon} = 0, \quad \operatorname{div} \boldsymbol{B}^{\epsilon} = 0, \quad \operatorname{curl} \boldsymbol{H}^{\epsilon} = \mathbf{0} \qquad \text{in } \Omega_{2\epsilon}, \tag{1b}$$

$$e(\boldsymbol{v}^{\epsilon}) = 0, \quad \operatorname{div} \boldsymbol{B}^{\epsilon} = 0, \quad \operatorname{curl} \boldsymbol{H}^{\epsilon} = \mathrm{R_m}\, \boldsymbol{v}^{\epsilon} \times \boldsymbol{B}^{\epsilon} \qquad \text{in } \Omega_{1\epsilon}, \tag{1c}$$

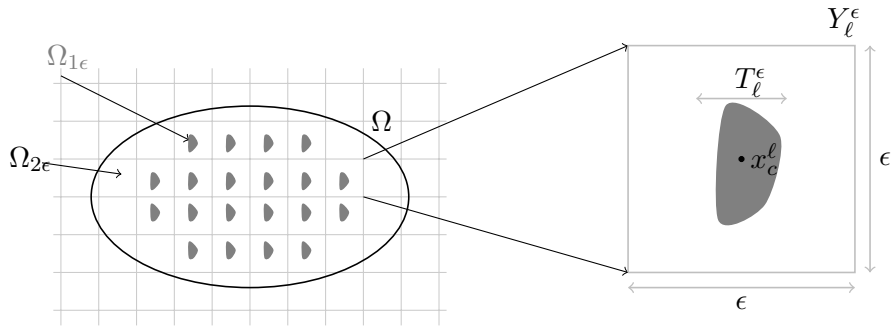

Figure 1: Schematic of the periodic suspension of rigid magnetizable particles in non-magnetizable fluid

where from (1c) the following compatibility conditions result

$$\operatorname{div} \mathrm{R_m}\, \boldsymbol{v}^\epsilon \times \boldsymbol{B}^\epsilon = 0, \quad \langle \mathrm{R_m}\, \boldsymbol{v}^\epsilon \times \boldsymbol{B}^\epsilon \cdot \boldsymbol{n} \mid 1 \rangle_{\mathrm{H}^{1/2}(\mathrm{S}_\ell^\epsilon), \mathrm{H}^{1/2}(\mathrm{S}_\ell^\epsilon)} = 0. \tag{2}$$

The interface and exterior boundary conditions are:

$$\begin{aligned} [\![\boldsymbol{v}^\epsilon]\!] = \boldsymbol{0}, \quad [\![\boldsymbol{B}^\epsilon \cdot \boldsymbol{n}]\!] = 0, \quad [\![\boldsymbol{n} \times \boldsymbol{H}^\epsilon]\!] = \boldsymbol{0} \qquad & \text{on } S_\ell^\epsilon, \\ \boldsymbol{v}^\epsilon = \boldsymbol{0}, \quad \boldsymbol{H}^\epsilon \cdot \boldsymbol{n} = \boldsymbol{c} \cdot \boldsymbol{n} \qquad & \text{on } \partial\Omega. \end{aligned} \tag{3}$$

Here $\boldsymbol{v}^\epsilon$ represents the fluid velocity field, p^ϵ the pressure, $e(\boldsymbol{v}^\epsilon)$ the strain rate, $\boldsymbol{n}$ the exterior normal to the particles, $\boldsymbol{H}^\epsilon$ the magnetic field, μ^ϵ is the magnetic permeability of the material with $\mu^\epsilon(\boldsymbol{x}) = \mu_1$ if $\boldsymbol{x} \in \Omega_{1\epsilon}$ and $\mu^\epsilon(\boldsymbol{x}) = \mu_2$ if $\boldsymbol{x} \in \Omega_{2\epsilon}$ with $0 < \mu_2 < \mu_1$, $\boldsymbol{B}^\epsilon$ is the magnetic induction $\boldsymbol{B}^\epsilon = \mu^\epsilon \boldsymbol{H}^\epsilon$, and $\boldsymbol{c}$ is an applied constant magnetic field on the exterior boundary of the domain Ω, $\partial\Omega$, $\boldsymbol{x}_c^\ell$ is the center of mass of the rigid particle T_ℓ^ϵ, α is the Alfven number, and $\mathrm{R_m}$ is the magnetic Reynolds number.

When the MR fluid is submitted to a magnetic field, the rigid particles are subjected to a force that makes them behave like a dipole aligned in the direction of the magnetic field. This force can be written in the form, $\boldsymbol{F}^\epsilon := -\frac{1}{2}\,|\boldsymbol{H}^\epsilon|^2\, \nabla\, \mu^\epsilon$, where $|\cdot|$ represents the standard Euclidean norm. The force can be written in terms of the Maxwell stress $\tau_{ij}^\epsilon = \mu^\epsilon\, H_i^\epsilon\, H_j^\epsilon - \frac{1}{2}\,\mu^\epsilon\, H_k^\epsilon\, H_k^\epsilon\, \delta_{ij}$ as $\boldsymbol{F}^\epsilon = \operatorname{div} \tau^\epsilon - \boldsymbol{B}^\epsilon \times \operatorname{curl} \boldsymbol{H}^\epsilon$. Since the magnetic permeability is considered constant in each phase, it follows that the force is zero in each phase. Therefore, we deduce that

$$\operatorname{div} \tau^\epsilon = \begin{cases} 0 & \text{if } \boldsymbol{x} \in \Omega_{2\epsilon} \\ \boldsymbol{B}^\epsilon \times \operatorname{curl} \boldsymbol{H}^\epsilon & \text{if } \boldsymbol{x} \in \Omega_{1\epsilon}. \end{cases} \tag{4}$$

Lastly, we remark that unlike the viscous stress σ^ϵ, the Maxwell stress is present in the entire domain Ω. Hence, we can write the balance of forces and torques for each particle as,

$$\begin{aligned} 0 &= \int_{S_\ell^\epsilon} \sigma^\epsilon \boldsymbol{n}\, ds + \alpha \int_{S_\ell^\epsilon} [\![\tau^\epsilon \boldsymbol{n}]\!]\, ds - \alpha \int_{T_\ell^\epsilon} \boldsymbol{B}^\epsilon \times \operatorname{curl} \boldsymbol{H}^\epsilon\, d\boldsymbol{x}, \\ 0 &= \int_{S_\ell^\epsilon} \sigma^\epsilon \boldsymbol{n} \times (\boldsymbol{x} - \boldsymbol{x}_c^\ell)\, ds + \alpha \int_{S_\ell^\epsilon} [\![\tau^\epsilon \boldsymbol{n}]\!] \times (\boldsymbol{x} - \boldsymbol{x}_c^\ell)\, ds \\ &\quad - \alpha \int_{T_\ell^\epsilon} (\boldsymbol{B}^\epsilon \times \operatorname{curl} \boldsymbol{H}^\epsilon) \times (\boldsymbol{x} - \boldsymbol{x}_c^\ell)\, d\boldsymbol{x}. \end{aligned} \tag{5}$$

Existence of a weak solution to the above model (1)–(5) relies [14] on Shinbrot's fixed point theorem [18] and certain a priori estimates for the velocity field $\boldsymbol{u}^\epsilon$ and the magnetic field $\boldsymbol{H}^\epsilon$, for sufficiently small $\mathrm{R_m}$.

2.2 Effective balance equations

The effective balance equations, for the above model for an MR fluid, were obtained in [15] as the limit when $\epsilon \to 0$ of the system (1)–(5) under the assumption of quasi-neutrality [6] using two–scale expansions and have the following form,

$$\begin{aligned}
&\operatorname{div}\left(\sigma^{hom}+\tau^{hom}\right)=\mathbf{0} \text{ in } \Omega,\\
&\sigma^{hom}+\tau^{hom}=\left(-\bar{p}^0+\frac{1}{d}\left(\beta_b-\beta_s\right)\left|\widetilde{\boldsymbol{H}}^0\right|^2\right) I+\nu_s\, e(\boldsymbol{v}^0)+\beta_s\,\widetilde{\boldsymbol{H}}^0\otimes\widetilde{\boldsymbol{H}}^0,\\
&\operatorname{div}\boldsymbol{v}^0=0 \text{ in } \Omega,\\
&\operatorname{div}\left(\mu^{hom}\,\widetilde{\boldsymbol{H}}^0\right)=0 \text{ in } \Omega,\\
&\operatorname{curl}\widetilde{\boldsymbol{H}}^0=\mathrm{R_m}\,\boldsymbol{v}^0\times\mu^{hom,s}\,\widetilde{\boldsymbol{H}}^0 \text{ in } \Omega,
\end{aligned} \tag{6}$$

with the boundary conditions:

$$\boldsymbol{v}^0=\mathbf{0} \text{ on } \partial\Omega, \quad \widetilde{\boldsymbol{H}}^0\cdot\boldsymbol{n}=\boldsymbol{c}\cdot\boldsymbol{n} \text{ on } \partial\Omega. \tag{7}$$

We remark that a necessary compatibility condition that resuts from (6) is that:

$$\operatorname{div}(\mathrm{R_m}\,\boldsymbol{v}^0\times\mu^{hom,s}\,\widetilde{\boldsymbol{H}}^0)=0 \text{ in } \Omega. \tag{8}$$

The effective stress tensor derived contains contribution both from the fluid and the magnetic field components, consisting an effective viscosity ν_s, and and four homogenized magnetic permeabilities, β_s and β_b, μ^{hom}, and $\mu^{hom,s}$ computed as the angular averaging of the tensors $\nu^{hom}_{ijm\ell}$, $\beta^{hom}_{ijm\ell}$, μ^{hom}_{ij}, and $\mu^{hom,s}_{ij}$ which all depend on the geometry of the suspension, the volume fraction, the magnetic permeability μ, the Alfven number α, and the particles distribution.

The effective coefficients $\nu^{hom}_{ijm\ell}$, $\beta^{hom}_{ijm\ell}$, μ^{hom}_{ik}, and $\mu^{hom,s}_{ik}$ are given by the formulas:

$$\nu^{hom}_{ijm\ell}=\int_{Y_f} 2\,e(\boldsymbol{B}^{ml}+\boldsymbol{\chi}^{ml}):e(\boldsymbol{B}^{ij}+\boldsymbol{\chi}^{ij})\,d\boldsymbol{y}, \tag{9}$$

$$\beta^{hom}_{ijm\ell}=\int_{Y_f} 2e(\boldsymbol{\xi}^{ml}):e(\boldsymbol{B}^{ij}+\boldsymbol{\chi}^{ij})d\boldsymbol{y}+\alpha\int_{Y_f}\mu A^{m\ell}:e(\boldsymbol{B}^{ij}+\boldsymbol{\chi}^{ij})d\boldsymbol{y}+\alpha\int_{Y}\mu A^{m\ell}_{ij}d\boldsymbol{y}, \tag{10}$$

$$\mu^{hom}_{ik}=\int_Y \mu\left(-\frac{\partial\phi^k}{\partial y_i}+\delta_{ik}\right)d\boldsymbol{y}, \tag{11}$$

and

$$\mu^{hom,s}_{ik}=\int_T \mu\left(-\frac{\partial\phi^k}{\partial y_i}+\delta_{ik}\right)d\boldsymbol{y}. \tag{12}$$

Here the effective coefficients are defined in terms of $\boldsymbol{\chi}^{m\ell},\boldsymbol{\xi}^{ml},\phi^\ell$ the solutions to the local problems formulated in the subsection below. We have also denoted $B^{ij}_k=\frac{1}{2}(y_i\,\delta_{jk}+y_j\,\delta_{ik})-\frac{1}{n}y_k\,\delta_{ij}$, and the fourth order tensor

$$A^{m\ell}_{ij}=\frac{1}{2}\left(A_{i\ell}\,A_{jm}+A_{j\ell}\,A_{im}-A_{mk}\,A_{\ell k}\,\delta_{ij}\right) \tag{13}$$

where $A_{i\ell}(\boldsymbol{y})=\left(-\frac{\partial\phi^\ell(\boldsymbol{y})}{\partial y_i}+\delta_{i\ell}\right)$.

2.3 Local problems

In this subsection we define the local problems to which the functions $\boldsymbol{\chi}^{m\ell}$, ϕ^{ℓ}, $\boldsymbol{\xi}^{ml}$ are solutions to.

First $\boldsymbol{\chi}^{m\ell}$ that enters in the definition of the homogenized viscosity $\nu^{hom}_{ijm\ell}$ and of the magnetic permeability $\beta^{hom}_{ijm\ell}$ is a solution to the following local problem,

$$\begin{aligned} -\frac{\partial}{\partial y_j}\varepsilon^{m\ell}_{ij} &= 0 \quad \text{in } Y_f, \\ \varepsilon^{m\ell}_{ij} &= -p^{m\ell}\delta_{ij} + 2\left(C_{ijm\ell} + e_{ijy}(\boldsymbol{\chi}^{m\ell})\right) \\ -\frac{\partial \chi^{m\ell}_i}{\partial y_i} &= 0 \quad \text{in } Y_f, \\ \left[\!\left[\boldsymbol{\chi}^{m\ell}\right]\!\right] &= 0 \quad \text{on } S\,, \\ C_{ijm\ell} + e_{ijy}(\boldsymbol{\chi}^{m\ell}) &= 0 \quad \text{in } T\,, \\ \boldsymbol{\chi}^{m\ell} \text{ is } Y-\text{periodic}, &\quad \widetilde{\boldsymbol{\chi}^{m\ell}} = \mathbf{0}, \end{aligned} \tag{14}$$

together with the balance of forces and torques,

$$\int_S \varepsilon^{m\ell}_{ij} n_j \, ds = 0, \quad \int_S \epsilon_{ijk}\, y_j\, \varepsilon^{m\ell}_{kp} n_p \, ds = 0, \tag{15}$$

where $C_{ijm\ell} = \dfrac{1}{2}(\delta_{im}\delta_{j\ell} + \delta_{i\ell}\delta_{jm}) - \dfrac{1}{n}\delta_{ij}\,\delta_{m\ell}$. We remark that if we define $B^{ij}_k = \frac{1}{2}(y_i\,\delta_{jk} + y_j\,\delta_{ik}) - \frac{1}{n} y_k\,\delta_{ij}$, then it immediately follows that $e_{ij}(\boldsymbol{B}^{m\ell}) = C_{ijm\ell}$.

The variational formulation of (14)-(15) is: Find $\boldsymbol{\chi}^{m\ell} \in \mathcal{U}$ such that

$$\int_{Y_f} 2\, e_{ij}(\boldsymbol{\chi}^{m\ell})\, e_{ij}(\boldsymbol{\phi} - \boldsymbol{\chi}^{m\ell})\, d\boldsymbol{y} = 0, \text{ for all } \boldsymbol{\phi} \in \mathcal{U}, \tag{16}$$

where $\mathcal{U}$ is the closed, convex, non-empty subset of $H^1_{per}(Y)^n$ defined by

$$\begin{aligned} \mathcal{U} = \Big\{ \boldsymbol{u} \in H^1_{\mathrm{per}}(Y)^n \mid \operatorname{div} \boldsymbol{u} = 0 \text{ in } Y_f, & e_{ij}(\boldsymbol{u}) = -C_{ijm\ell} \text{ in } T, \\ & [\![\boldsymbol{u}]\!] = \mathbf{0} \text{ on } S, \widetilde{\boldsymbol{u}} = \mathbf{0} \text{ in } Y \Big\}. \end{aligned} \tag{17}$$

The existence and uniqueness of a solution follows from classical theory of variational inequalities.

Second the local problem defining ϕ^{ℓ} which enters in the definition of all the effective magnetic permeabilities $\beta^{hom}_{ijm\ell}$, $\mu^{hom,s}_{ik}$ and μ^{hom}_{ik} is,

$$\begin{aligned} -\frac{\partial}{\partial y_i}\left(\mu\left(-\frac{\partial \phi^{\ell}}{\partial y_i} + \delta_{i\ell}\right)\right) &= 0 \quad \text{in } Y, \\ \left[\!\left[\mu\left(-\frac{\partial \phi^{\ell}}{\partial y_i} + \delta_{i\ell}\right) n_i\right]\!\right] &= 0 \quad \text{on } S\,, \\ \phi^{\ell} \text{ is } Y-\text{periodic}, &\quad \widetilde{\phi^{\ell}} = 0. \end{aligned} \tag{18}$$

or in variational form: Find $\phi^k \in \mathcal{W} = \left\{ w \in H^1_{per}(Y) \mid \widetilde{w} = 0 \right\}$ such that,

$$\int_Y \mu \, \frac{\partial \phi^k}{\partial y_i} \, \frac{\partial v}{\partial y_i} \, d\boldsymbol{y} = \int_Y \mu \, \frac{\partial v}{\partial y_k} \, d\boldsymbol{y} \text{ for any } v \in \mathcal{W}. \tag{19}$$

And the third local problem defining $\boldsymbol{\xi}^{ml}$, which enters in the definition of the homogenized permeability $\beta^{hom}_{ijm\ell}$ is

$$\begin{aligned} -\frac{\partial}{\partial y_j}\Sigma^{m\ell}_{ij} &= 0 \quad \text{in } Y_f, \\ \Sigma^{m\ell}_{ij} &= -\pi^{m\ell}\delta_{ij} + 2\, e_{ijy}(\boldsymbol{\xi}^{m\ell}) \\ -\frac{\partial \xi^{m\ell}_i}{\partial y_i} &= 0 \quad \text{in } Y_f, \\ \left[\!\left[\boldsymbol{\xi}^{m\ell}\right]\!\right] &= 0 \quad \text{on } S\,, \\ e_{ijy}(\boldsymbol{\xi}^{m\ell}) &= 0 \quad \text{in } T\,, \\ \boldsymbol{\xi}^{m\ell} \text{ is } Y-&\text{periodic}, \quad \widetilde{\boldsymbol{\xi}^{m\ell}} = 0, \end{aligned} \tag{20}$$

with balance of forces and torques,

$$\int_S \Sigma^{m\ell}_{ij}\, n_j \, ds = 0, \quad \int_S \epsilon_{ijk}\, y_j \, \left(\Sigma^{m\ell}_{kp} + \alpha \left[\!\left[\mu A^{m\ell}_{kp} \right]\!\right] \right) \, n_p \, ds = 0. \tag{21}$$

We can formulate (20)–(21) variationally as: Find $\boldsymbol{\xi}^{m\ell} \in \mathcal{V}$ such that

$$\int_{Y_f} 2\, e_{ijy}(\boldsymbol{\xi}^{m\ell})\, e_{ijy}(\boldsymbol{\phi})\, d\boldsymbol{y} + \int_Y A^{m\ell}_{ij}\, e_{ijy}(\boldsymbol{\phi})\, d\boldsymbol{y} = 0, \text{ for all } \boldsymbol{\phi} \in \mathcal{V}, \tag{22}$$

where $\mathcal{V} = \left\{ \boldsymbol{v} \in H^1_{\rm per}(Y)^d \mid \operatorname{div} \boldsymbol{v} = 0 \text{ in } Y_f,\, e_y(\boldsymbol{u}) = 0 \text{ in } T,\, [\![\boldsymbol{v}]\!] = \boldsymbol{0} \text{ on } S,\, \widetilde{\boldsymbol{v}} = \boldsymbol{0} \text{ in } Y \right\}$, is a closed subspace of $H^1_{\rm per}(Y)^d$. Existence and uniqueness follows from an application of the Lax–Milgram lemma. These equations indicate the contribution of the magnetic field and the solution $\boldsymbol{\xi}^{m\ell}$ depends, through the balance of forces and torques on the solution of the local problem (19) and the effective magnetic permeability of the composite. We have defined the fourth order tensor

$$A^{m\ell}_{ij} = \frac{1}{2}\, \left(A_{i\ell}\, A_{jm} + A_{j\ell}\, A_{im} - A_{mk}\, A_{\ell k}\, \delta_{ij} \right) \tag{23}$$

where $A_{i\ell}(\boldsymbol{y}) = \left(-\frac{\partial \phi^\ell(\boldsymbol{y})}{\partial y_i} + \delta_{i\ell} \right)$ We remark that the only driving force that makes the solution $\boldsymbol{\xi}^{m\ell}$ non trivial in (22) is the rotation induced by the magnetic field through the fourth order tensor $A^{m\ell}_{ij}$.

3 Computation of the local solutions: Penalization and viscosity methods

The goal of this section is to carry out calculations, using the finite element method, the effective magnetic coefficients $\beta^{hom}_{ijk\ell}$ that characterizes the magnetorheological effect in the presence of different geometrical realizations of chain particles.

In order to compute $\beta^{hom}_{ijk\ell}$ we must compute the local solutions $\boldsymbol{\chi}^{m\ell}$, $\boldsymbol{\xi}^{m\ell}$, ϕ^k of the local problems (16), (22), and (19) respectively.

For all local problems, $\boldsymbol{\chi}^{m\ell}$, $\boldsymbol{\xi}^{m\ell}$, and ϕ^{ℓ} we briefly describe how to implement the penalization method to enforce the rigid body motion of the particle and how to implement the viscosity method to enforce a zero average over the unit cell Y so that the local solutions can be uniquely determined.

We will discuss here how to implement the methods for the local solution $\boldsymbol{\chi}^{m\ell}$ of (16) with the approximations of the other local solutions being similar. The solution to (16) can be classified as a minimum of the energy functional $\mathcal{J}$ in the following way: Find $\boldsymbol{\chi}^{m\ell} \in \mathcal{U}$ such that,

$$\mathcal{J}(\boldsymbol{\chi}^{m\ell}) = \min_{\boldsymbol{w}\in H^1_{\mathrm{per}}(Y)^d} \mathcal{J}(\boldsymbol{w}), \tag{24}$$

where $\mathcal{J}(\boldsymbol{w}) = \int_{Y_f} |e(\boldsymbol{w})|^2 \, d\boldsymbol{y} + \mathbb{I}_{\mathcal{U}}(\boldsymbol{w})$. We approximate the solution to (24) by the following sequence of vector fields: Find $\boldsymbol{\chi}^{m\ell}_{\lambda} \in \overline{\mathcal{U}}$ such that,

$$\mathcal{J}^{\lambda}(\boldsymbol{\chi}^{m\ell}_{\lambda}) = \min_{\boldsymbol{u}\in H^1_{\mathrm{per}}(Y)^d} \mathcal{J}^{\lambda}(\boldsymbol{u}), \tag{25}$$

where

$$\mathcal{J}^{\lambda}(\boldsymbol{u}) = \int_{Y_f} |e(\boldsymbol{u})|^2 \, d\boldsymbol{y} + \frac{1}{2\lambda} \int_{Y_s} \left| e\Big(\boldsymbol{u} + \boldsymbol{B}^{m\ell}\Big) \right|^2 d\boldsymbol{y} + \mathbb{I}_{\overline{\mathcal{U}}}(\boldsymbol{u}), \tag{26}$$

and

$$\overline{\mathcal{U}} = \Big\{ \boldsymbol{u} \in H^1_{\mathrm{per}}(Y)^d \mid \operatorname{div} \boldsymbol{u} = 0 \text{ in } Y_f, [\![\boldsymbol{u}]\!] = \boldsymbol{0} \text{ on } S, \widetilde{\boldsymbol{u}} = \boldsymbol{0} \text{ in } Y \Big\}. \tag{27}$$

It is clear that $\mathcal{J}^{\lambda}$ is monotone in λ and hence Γ-converges in w-$H^1_{\mathrm{per}}(Y)^d$ to $\mathcal{J}$ as $\lambda \to 0$. To impose a zero average of the solution we use the viscosity method to approximate $\boldsymbol{\chi}^{m\ell}_{\lambda}$ by $\boldsymbol{\chi}^{m\ell}_{\lambda,\delta}$ unique minimum of the following problem: Find $\boldsymbol{\chi}^{m\ell}_{\lambda,\delta} \in \hat{\mathcal{U}}$ such that,

$$\mathcal{J}^{\lambda,\delta}(\boldsymbol{\chi}^{m\ell}_{\lambda,\delta}) = \min_{\boldsymbol{z}\in H^1_{\mathrm{per}}(Y)^d} \mathcal{J}^{\lambda,\delta}(\boldsymbol{z}), \tag{28}$$

where

$$\begin{aligned} \mathcal{J}^{\lambda,\delta}(\boldsymbol{z}) = &\int_{Y_f} |e(\boldsymbol{z})|^2 \, d\boldsymbol{y} + \frac{1}{2\lambda} \int_{Y_s} \left| e\Big(\boldsymbol{z} + \boldsymbol{B}^{m\ell}\Big) \right|^2 d\boldsymbol{y} \\ &+ \frac{\delta}{2} \int_{Y} |\boldsymbol{z}|^2 \, d\boldsymbol{y} + \mathbb{I}_{\hat{\mathcal{U}}}(\boldsymbol{z}), \end{aligned} \tag{29}$$

and

$$\hat{\mathcal{U}} = \Big\{ \boldsymbol{u} \in H^1_{\mathrm{per}}(Y)^d \mid \operatorname{div} \boldsymbol{u} = 0 \text{ in } Y_f, [\![\boldsymbol{u}]\!] = \boldsymbol{0} \text{ on } S \Big\}. \tag{30}$$

By computing the Gateaux derivative of $\mathcal{J}^{\lambda,\delta}$ we obtain the following weak formulation,

$$\begin{aligned} \int_{Y_f} 2\, e(\boldsymbol{\chi}^{m\ell}_{\lambda,\delta}) : e(\boldsymbol{\phi}) \, d\boldsymbol{y} + \frac{1}{\lambda} \int_{Y_s} e\Big(\boldsymbol{\chi}^{m,\ell}_{\lambda,\delta} + \boldsymbol{B}^{m\ell}\Big) : e(\boldsymbol{\phi}) \, d\boldsymbol{y} \\ + \delta \int_{Y} \boldsymbol{\chi}^{m\ell}_{\lambda,\delta} \cdot \boldsymbol{\phi} \, d\boldsymbol{y} = 0, \end{aligned} \tag{31}$$

for any test function $\boldsymbol{\phi} \in \hat{\mathcal{U}}$. Using any constant as a test function we can recover that $\widetilde{\boldsymbol{\chi}_{\lambda}^{m\ell}} = \mathbf{0}$. Again, due to the monotonicity of $\mathcal{J}^{\lambda,\delta}$ in δ we have that $\mathcal{J}^{\lambda,\delta}$ Γ-converges in w-$H^1_{\text{per}}(Y)^d$ to $\mathcal{J}^{\lambda}$. Hence, we have,

$$\limsup_{\lambda\to 0}\limsup_{\delta\to 0}\mathcal{J}^{\lambda,\delta}(\boldsymbol{\chi}_{\lambda,\delta}^{m\ell}) \leq \mathcal{J}(\boldsymbol{\chi}^{m\ell}). \tag{32}$$

Using a diagonalization argument [1], there exists a map $\delta \mapsto \lambda(\delta)$ such that $\lim_{\delta\to 0}\lambda(\delta) = 0$ and

$$\limsup_{\delta\to 0}\mathcal{J}^{\lambda(\delta),\delta}(\boldsymbol{\chi}_{\lambda(\delta),\delta}^{m\ell}) \leq \limsup_{\lambda\to 0}\limsup_{\delta\to 0}\mathcal{J}^{\lambda,\delta}(\boldsymbol{\chi}_{\lambda,\delta}^{m\ell}). \tag{33}$$

A similar argument exists for the $\liminf$ expression but the inequality is reversed. Hense, the theory of Γ-convergence guarantees that our approximate solutions converge to the desired solutions. For more details the one can consult the works in [1], [13, Appendix A].

Thus using the penalization and viscosiy methods we can compute the local solution $\boldsymbol{\xi}^{m\ell}$. In Fig. 2 and Fig. 3 we plot $\boldsymbol{\xi}^{m\ell}$ in the case of circular iron particles of 15% volume fraction and $\alpha = 1$ for different geometrical **chain** realizations.

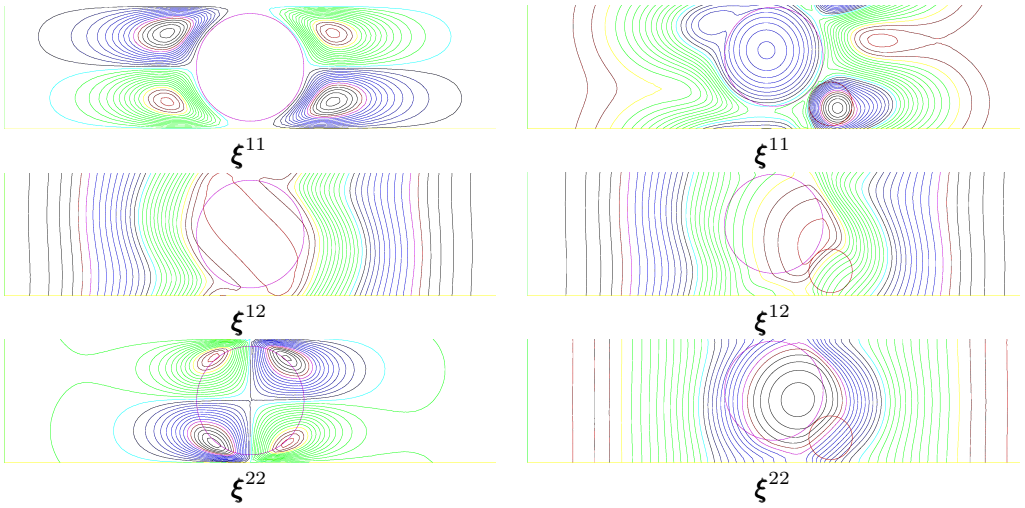

Figure 2: Streamlines of the solution of the local problems for circular iron particles of 15% volume fraction and $\alpha = 1$ for different geometrical **chain** realizations. The left row showcases the streamlines for the local solution $\boldsymbol{\xi}^{m\ell}$ in (22) for a single particle while the row on the right showcases the streamlines for two particles.

4 Effective magnetic coefficient for different geometrical realizations

Unlike regular suspensions for which the effective properties are dependent only on fluid viscosity, particle geometry, and volume fraction, for magnetorheological fluids of significance is also the particles' distribution. The magnetic field polarizes the particles, which align in the field direction, to form *chains* and *columns* and that contributes significantly to the increase of the yield stress [2], [19], [22]. In the work of [15] it was shown that in the presence of chain structures, the magnetorheological effect increases non-linearly with the volume fraction (see Fig. 4). The choice of the periodic unit cell, as well as the geometry and distribution of particles, can lead to different *chain structures* and hence different effective properties.

In all computations we have used a regular, symmetric, triangular mesh. For the $2 \times \frac{1}{2}$ periodic unit cell, we used 100×20 $P1$ elements for the rectangle and 100 $P1$ elements for the circular particle. Other geometries where the particle is an ellipse, for instance, present an interesting case on their own. Ellipses have a priori a

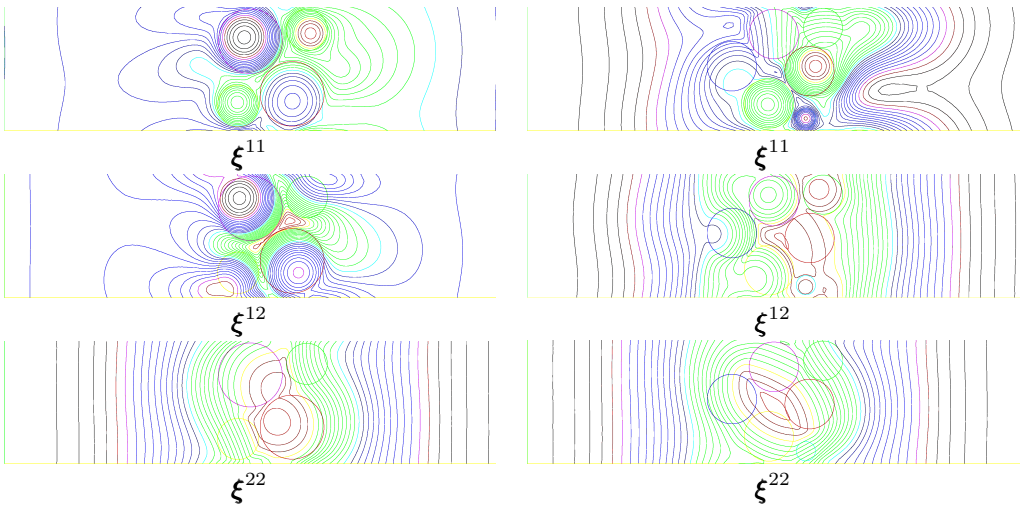

Figure 3: Streamlines of the solution of the local problems for circular iron particles of 15% volume fraction and $\alpha = 1$ for different geometrical **chain** realizations. The left row showcases the streamlines for the local solution $\boldsymbol{\xi}^{m\ell}$ in (22) for a four particles while the row on the right showcases the streamlines for six particles.

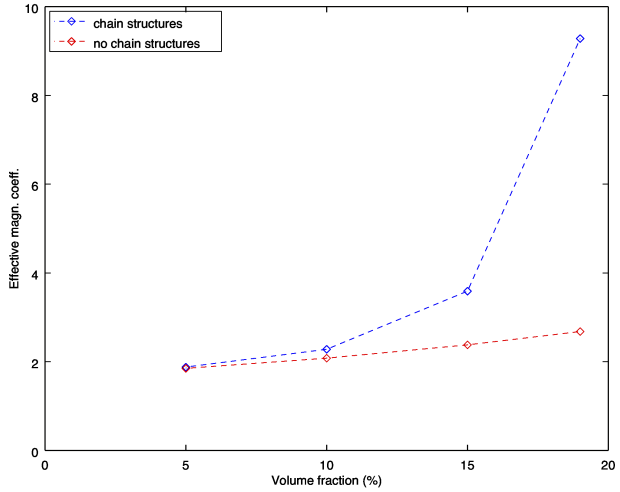

Figure 4: Effective magnetic coefficient β_s plotted against volume fractions of 5%, 10%, 15%, and 19% for circular iron particles. The **red** color curve showcases the increase of the effective magnetic coefficient β_s under uniform particle distribution while the **blue** color curve showcases the increase of the effective magnetic coefficient β_s in the presence of **chain structures**

.

preferred direction i.e. they are anisotropic and as result the effective coefficients will be anisotropic. Hence, when one discusses *chain structures* of ellipses the *angle orientation* must be taken into account. We will not discuss such cases here.

We remark that in the two dimensional setting, the tensors entries $C_{ijmm} = 0$ and $\boldsymbol{B}^{mm} = \mathbf{0}$. As a consequence, of the linearity of the local problem (14), we have $\boldsymbol{\chi}^{mm} = \mathbf{0}$. Hence, $\nu_{mmii} = 0$ which implies that $\nu_b = 0$. Using a similar argument, we can similarly show that $\beta_{mmii} = 0$ which implies that $\beta_b = 0$.

The relative magnetic permeability of the iron particle (99.95% pure) was fixed through out to be 2×10^5 while that of the fluid was set to 1 [4]. All the calculations were carried out using the software `FreeFem++` [7].

For particles with fixed volume fraction of 15% we compute the effective magnetic coefficient β_s for different geometrical chain realizations. By breaking a single large particle into smaller particles we achieve two objectives: 1) we obtain different chain structures formed from clustered particles, 2) we increase the surface area of the mag-

netic material while keeping the volume fraction the same. We considered four different geometrical realizations of chain structures with a single particle, two particles, four particles, and six particles as in Fig. 2 and Fig. 3.

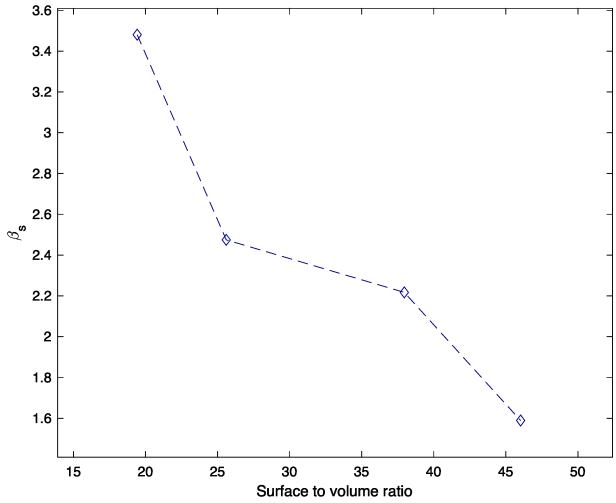

Figure 5: Effective magnetic coefficient β_s plotted against surface to volume ratio for different realizations of chain particles with constant volume fraction of 15%.

Fig. 5 showcases the effective coefficient β_s introduced in (6) versus the surface to volume ratio for different chain structures introduced in Fig. 2 and Fig. 3. We can readily observe that as the surface to volume ratio increases the effective magnetic coefficient decreases leading to a weaker magnetorheological effect for the overall suspension.

5 Conclusions

Using the homogenization method we have obtained, starting from a hybrid model for a suspension of rigid magnetizable particles in a newtonian fluid, a model (6) – (7). The model has several novel features. First it is a coupled system, and not partially uncoupled as most in the literature; so one cannot solve the Maxwell equations separately from the flow. Second, the pressure term in the constitutive equation in (6) exhibits a magnetic component, which is to our knowledge a novel in the magnetorheological literature. Third, unlike in phenomenological approaches the coefficients of the various terms in the constitutive equation are defined precisely and depend on the material properties, geometry and applied fields, and thus can be computed numerically for different materials and structures. Forth, it is to be remarked that the Maxwell equations in (6) have different magnetic permeabilities, which is again a novel part.

The model we obtained allows us to simulate the chain formation, which is the essence of the magnetorheological effect: the fact that the particles organize in chain structures is responsible for the non-newtonian behavior of these materials, once a magnetic field is applied. In this paper we emphasise two phenomena. We show the nonlinearity of the effective magnetic coefficient β_s in the presence of chains vs. uniform distribution as the particle volume fraction increases, and this translates in the increase of the apparent yield stress [15]. We also show the importance of total particle surface area as the value of β_s decreases by increasing the surface area and keeping the volume fraction constant.

References

[1] H. Attouch, *Variational convergence for functions and operators*, Boston: Pitman Advance Pub. Program, 1984.

[2] G. Bossis, S. Lacis, A. Meunier, and O. Volkova, *Magnetorheological fluids*, J. Magnet. Magnetic. Mat. **252** (2002), 224–228.

[3] I. A. Brigadnov and A. Dorfmann, *Mathematical modelling of magnetorheological fluids*, Continuum Mech. Thermodyn. (2005), 29–42.

[4] E. H. Condon and H. Odishaw, *Handbook of physics*, New York, McGraw-Hill, 1958.

[5] J. de Vincente, D. J. Klingenberg, and R. Hidalgo-Alvarez, *Magnetorheological fluids: a review*, Soft Matter **7** (2011), 3701–3710.

[6] G. Duvaut and J.-L. Lions, *Les inéquations en mécanique et en physique*, Travaux Recherches Math., Dunod, Paris, 1972.

[7] F. Hecht, *New development in* `freefem++`., J Numer Math **20** (2012), 251–265.

[8] T. Levy, *Suspension de particules solides soumises á des couples*, J. Méch. Théor. App. **Numéro spécial** (1985), 53–71.

[9] T. Levy and R. K. T. Hsieh, *Homogenization mechanics of a non-dilute suspension of magnetic particles*, Int. J. Engng. Sci **26** (1988), 1087–1097.

[10] R. Lipton and B. Vernescu, *Variational methods, size effects and extremal microgeometries for elastic composites with imperfect interface*, Math. Mod. Meth. Appl. S. **5(8)** (1995), 1139–1173.

[11] ———, *Composites with imperfect interface*, Proc. R. Soc. Lond. A **452** (1996), 329–358.

[12] J. Liu, G. A. Flores, and R. Sheng, *In-vitro investigation of blood embolization in cancer treatment using magnetorheological fluids*, J. Magn. Magn. Mater. **225** (2001), no. 1-2, 209–217.

[13] G. Nika, *Multiscale analysis of emulsions and suspensions with surface effects*, Ph.D. thesis, Worcester Polytechnic Institute, 2016.

[14] G. Nika and B. Vernescu, *Asymptotics for a class of nonlinear magnetorheological composites*, (in preparation).

[15] ———, *Multiscale modeling of magnetorheological suspensions*, Z. Angew. Math. Phys. **71** (2020), no. 1, 1–19.

[16] J. Perlak and B. Vernescu, *Constitutive equations for electrorheological fluids*, Rev. Roumaine Math. Pures Appl. **45** (2000), 287–297.

[17] J. Rabinow, *The magnetic fluid clutch*, AIEE Trans. **67** (1948), no. 17-18, 1308.

[18] M. Shinbrot, *A fixed point theorem, and some applications*, Arch. Rational Mech. Anal. **17** (1964), 255–271.

[19] R. Tao, *Super-strong magnetorheological fluids*, J. Phys.: Condens. Matter **13** (2001), 979–999.

[20] D. Thapa, V. R. Palkar, M. B. Kurup, and S. K. Malik, *Properties of magnetite nanoparticles synthesized through a novel chemical route*, Materials Letters **58** (2004), 2692–2694.

[21] B. Vernescu, *Multiscale analysis of electrorheological fluids*, Inter. J. Modern Physics B **16** (2002), 2643–2648.

[22] W.M. Winslow, *Induced fibration of suspensions*, J. Appl. Phys. **20** (1949), 1137–1140.